Journal of Renewable Energy and Environment

Research Article

Journal Homepage: www.jree.ir

Numerical Study of Curved-Shape Channel Effect on Performance and Distribution of Species in a Proton-Exchange Membrane Fuel Cell: Novel Structure

Tuhid Pashaee Golmarz, Sajad Rezazadeh*, Narmin Bagherzadeh

Department of Mechanical Engineering, Urmia University of Technology, Urmia, Iran.

PAPER INFO

Paper history:
Received 15 December 2018
Accepted in revised form 20 March 2019

Keywords:
PEM Fuel Cell
Flow Channel Shape
Mass Transport
Performance

ABSTRACT

In this paper, a three-dimensional, single-phase proton-exchange membrane fuel cell (PEMFC) is studied numerically. Finite volume method was used for solving the governing equations and, consequently, the numerical results were validated by comparing them with experimental data, which showed good agreement. The main objective of this work is to investigate the effect of a novel gas channel shape- by applying sinusoidal gas channel- on the cell performance and mass transport phenomena. Some parameters such as oxygen consumption, water production, protonic conductivity, and temperature distribution for two cell voltages were studied, and the results were compared with respect to conventional and new models. The results indicated that the new novel model showed better performance than the conventional model, especially at low cell voltages, causing an increase in oxygen consumption and water production. Therefore, based on a number of investigated relations, a higher rate of current density was obtained, thus enhancing the fuel cell performance. This is because the incoming species path to the gas channels in the new model becomes longer. Therefore, the diffusion of the species toward the electrochemical reaction area increased.

1. INTRODUCTION

Fuel cells are devices that electrochemically convert the chemical energy of gaseous or liquid reactants into electrical energy. In a battery, the reactants are prevented from chemical reaction by separating them with an electrolyte, which is in contact with electro-catalytically active porous electrode structures. Apart from effectively separating the fuel and air, the electrolyte mediates the electrochemical reactions taking place at the electrodes by conducting a specific ion at very high rates during the operation of the fuel cell. In the simplest case of a fuel cell, a proton or oxide ion current is driven through the electrolyte and parts of the heterogeneous electrode structures. This type operates with hydrogen (fuel) and oxygen (air) as reacting gases [1].

Many researchers concentrated on different aspects of the fuel cell. Bernardi and Verbrugge [2, 3] studied an isothermal model that provides precious information about the physics of the electrochemical reactions and transport phenomenon in a fuel cell. Fuller and Newman [4] published a model of the membrane electrode assembly (MEA), which is based on concentration solution theory for the membrane and accounts for thermal effects. Nguyen and White [5] investigated an isothermal model. They focused on the effect of electro osmosis drag force on water transport through membrane and studied heat transfer from the solid phase to the gas phase.

Dutta et al. suggested the first 3D for PEMFC [6]. Berning et al. developed steady-state, 3-D, non-isothermal models to predict PEMFC behavior [7].

Yang et al. [8] improved the performance of PEMFC. In recent years, modern numerical methods have been used to investigate the performance improvement of PEMFC. Akbari et al. [9] used lattice Boltzmann method to indicate the water droplet dynamic behavior. It is necessary to understand these parameters and their effects on cell performance. Carral et al. [10] applied a finite element technique to simulate PEMFC stack.

Ahmadi et al. [11] numerically and experimentally studied a PEM fuel cell. Their results indicated that the proficiency of cell was enhanced by increasing the operating pressure. They also investigated GDL geometrical configuration effect on PEM fuel cell performance. The results showed a noticeable increase in current density at the similar cell voltages, compared with the base model.

Rezazadeh et al. [12] developed a three-dimensional and single-phase CFD model of a PEMFC with both gas distribution flow channels and the Membrane Electrode Assembly (MEA). They studied operating pressure effect in their paper. In addition, the effect of Gas Diffusion Layers (GDLs) geometrical configuration on cell performance showed that the observed model, with prominent GDLs, enhanced the cell performance, compared with the conventional model. While research and innovation in the field of fuel cells have been conducted, these systems and their applications are still extremely complex and expensive and are not proper for commercial use. Important aims of recent developments are concentrated on the cost reduction and large volume manufacturing of the catalyst layers, membranes, and bipolar plates.

The present work is a 3-D numerical study of novel-curved-channel effect on the performance and species distribution in a PEM fuel cell. Some important parameters such as species mass fractions, cell temperature, anode, and cathode overpotential were shown and compared by a simple model in more detail.

*Corresponding Author's Email: sor.mems@gmail.com (S. Rezazadeh)

The numerical results revealed that the new model operated better and showed higher performance.

2. MATHEMATICAL MODEL

Figures 1 and 2 show a schematic of a single cell of a PEMFC (base model). It is made of two porous electrodes, a polymer electrolyte membrane, a two-catalyst layer, and two-gas distributor plates. The membrane is sandwiched between the gas channels.

The present non-isothermal model includes some assumptions. The following simplifications have been applied for governing equation:

- All gases are ideal gas mixture.
- The GDLs and catalyst layers are homogeneously porous.
- The flow is assumed to be incompressible and laminar because of low-pressure gradients and velocities.
- The volume of liquid-phase water in the domain is not notable; thus, the flow field is single phase.

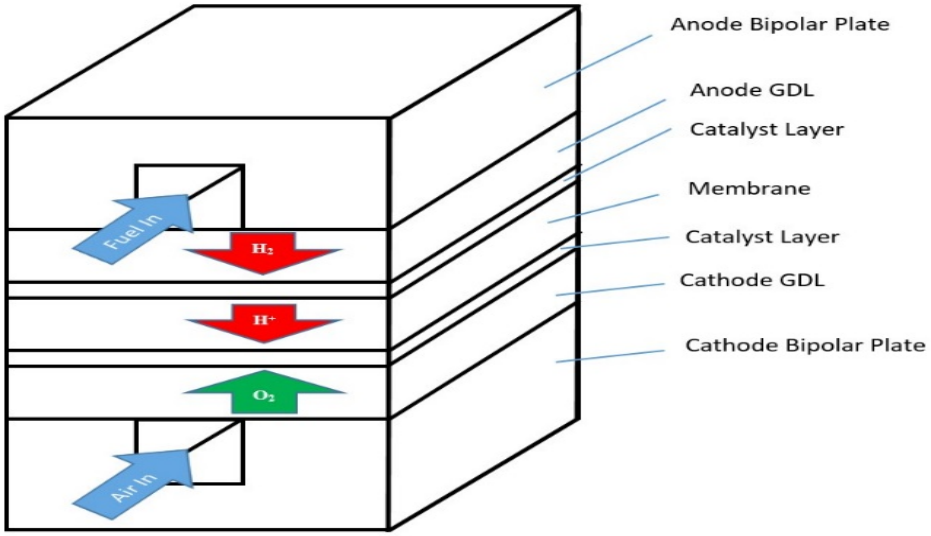

Figure 1. schematic of a PEMFC (base case).

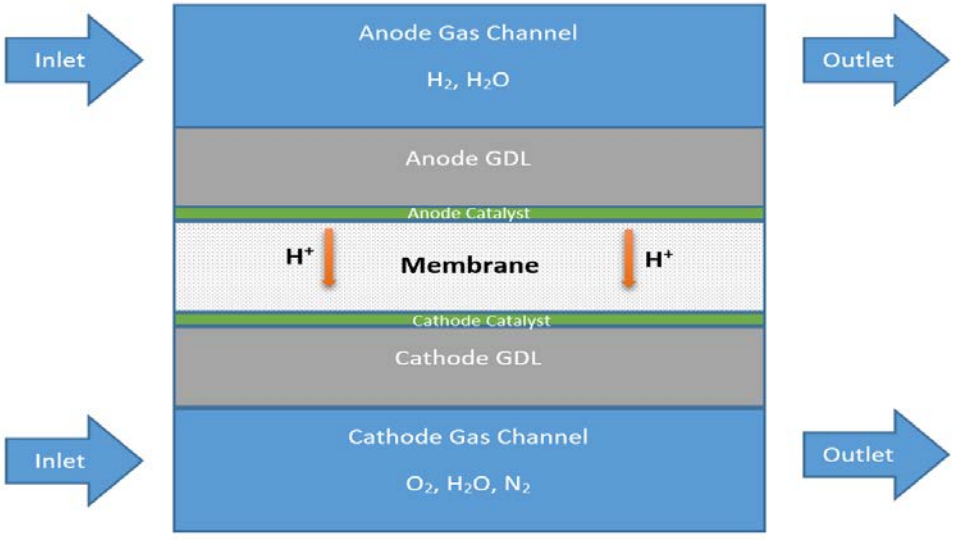

Figure 2. PEMFC in lateral view.

3. GOVERNING EQUATIONS

In this paper, a single domain model formulation was used for the governing equations. These governing equations consist of mass conservation, momentum, species, and charge equations, which can be written as follows:

$$(\nabla.\rho\mathbf{u}) = 0 \tag{1}$$

$$\frac{1}{(\varepsilon^{eff})^2}\nabla.(\rho\mathbf{uu}) = -\nabla P + \nabla.(\mu\nabla\mathbf{u}) + S_u \tag{2}$$

$$\nabla.(\mathbf{u}C_K) = \nabla.\left(D_K^{eff}\nabla C_K\right) + S_K \tag{3}$$

$$\nabla.\left(\kappa_e^{eff}\nabla\Phi_e\right) + S_\Phi = 0 \tag{4}$$

$$\nabla.(\rho uT) = \nabla.(\lambda_{eff}\nabla T) + S_T \tag{5}$$

In Equation (1), the mixture density is denoted by ρ. ε is the effective porosity entrant porous inductor, and the viscosity of the gas mixture in the momentum equation is denoted by μ in equation (2). S_u is the source of momentum equation term and is used to describe Darcy's drag for flow through porous gas diffusion layers and catalyst layers. More information about the governing equations and source terms is available in references [13-20].

4. BOUNDARY CONDITION

The mentioned governing equations are solved by using the boundary condition, as shown in Table 1.

5. MODEL VALIDATION

In order to verify the model, numerical results of the base case are compared with the experimental data presented by Ticianelli et al. [13], as shown in figure 3a, where there is a favorable agreement between them.

Fuel cell operating condition and geometric parameters are shown in Table 2. It is used in a fully humidified inlet condition for anode and cathode. The transfer current at anode and cathode can be described by Tafel equations [11].

Table 1. Boundary condition of fuel cell.

Boundary condition	The location
$u = u_{in}, T = T_{in}, v = 0, C_{H2} = C^{a}_{H2,in}\ ,\ C_{H2O} = C^{a}_{H2O}$	Anode channel inlet
$u = u_{in}, T = T_{in}, v = 0, C_{O2} = C^{c}_{O2,in}\ ,\ C_{N2} = C^{c}_{N2}$	Cathode channel inlet
$\frac{\partial u}{\partial x} = \frac{\partial v}{\partial x} = \frac{\partial w}{\partial z} = \frac{\partial T}{\partial x} = 0$	Anode and cathode channel exit
$\frac{\partial u}{\partial y}_{h_1^-} = \varepsilon_{eff,}GDL\frac{\partial u}{\partial y}_{h_1^+}, \frac{\partial v}{\partial y}_{h_1^-} = \varepsilon_{eff,}GDL\frac{\partial v}{\partial y}_{h_1^+}, \frac{\partial w}{\partial y}_{h_1^-} = \varepsilon_{eff,}GDL\frac{\partial w}{\partial y}_{h_1^+}$	Gas channel and GDL interface
$\varepsilon_{eff,}GDL\frac{\partial u}{\partial y}_{h_2^-} = \varepsilon_{eff,}CL\frac{\partial u}{\partial y}_{h_2^+}$ $\varepsilon_{eff,}GDL\frac{\partial u}{\partial y}_{h_2^-} = \varepsilon_{eff,}CL\frac{\partial u}{\partial y}_{h_2^+}$ $\varepsilon_{eff,}GDL\frac{\partial u}{\partial y}_{h_2^-} = \varepsilon_{eff,}CL\frac{\partial u}{\partial y}_{h_2^+}$	GDL and catalyst layer interface
$u = v = w = Ci = 0$	Catalyst layer and membrane interface
$u = v = w = Ci = 0, T_{surface} = 353K$	Top wall Of channel
$u = w = 0, T_{surface} = T_{wall}$	Bottom wall Of channel
$\phi_{sol} = 0\ , \frac{\partial \phi_{mem}}{\partial y} = 0$	Anode bipolar
$\phi_{sol} = V_{cell}\ , \frac{\partial \phi_{mem}}{\partial y} = 0$	Cathode bipolar
$\frac{\partial \phi_{mem}}{\partial x} = 0, \frac{\partial \phi_{mem}}{\partial z} = 0, \frac{\partial \phi_{sol}}{\partial x} = 0, \frac{\partial \phi_{sol}}{\partial z} = 0$	External surfaces

Table 2. Geometrical parameters and operating conditions [13].

Parameter	Value
Gas channel length	0.05 m
Gas channel width and	0.001 m
Cell width	0.002 m
Gas diffusion layer thickness	0.00026 m
Catalyst layer thickness	0.0000129 m
Membrane thickness	0.00023 m
Cell temperature	353.15 K
Anode pressure	3 atm
Cathode pressure	5 atm

In this model, the structured meshes are used and, in catalyst layers where the electro chemical reactions occur, the meshes are finer. In addition, grid independence test was implemented and, finally, the optimum number of meshes was chosenf (Figure 3b). According to the results, 240000 and 480000 cells have approximately the same output; therefore, for low computation time and fast convergence, 240000 cells were chosen as the best and useful ones.

Figures 4 to 7 demonstrate O_2, H_2o, current density, and temperature distributions through the cell width for four cross sections on interface between cathode catalyst and membrane layer in 10, 20, 30, and 40 mm in Z direction for the base model.

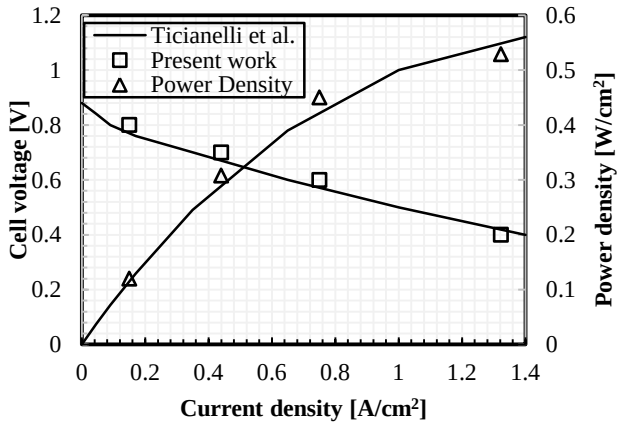

(a)

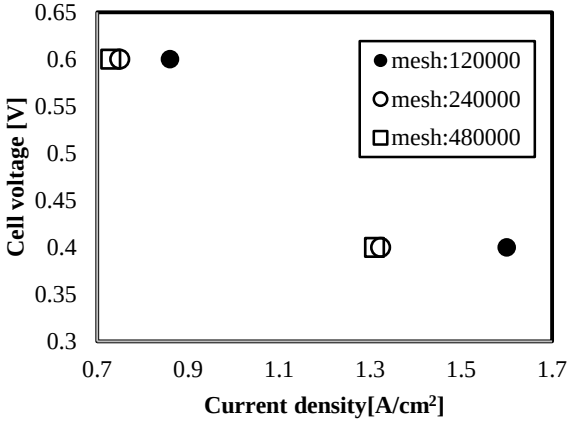

(b)

Figure 3. a) comparison with experimental data; b) grid independency.

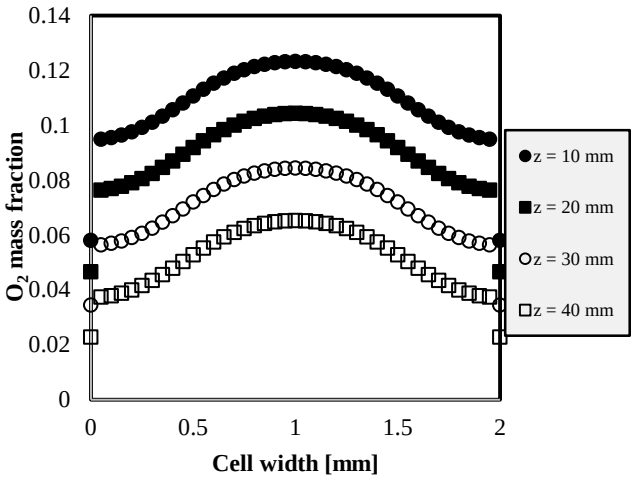

Voltage = 0.4

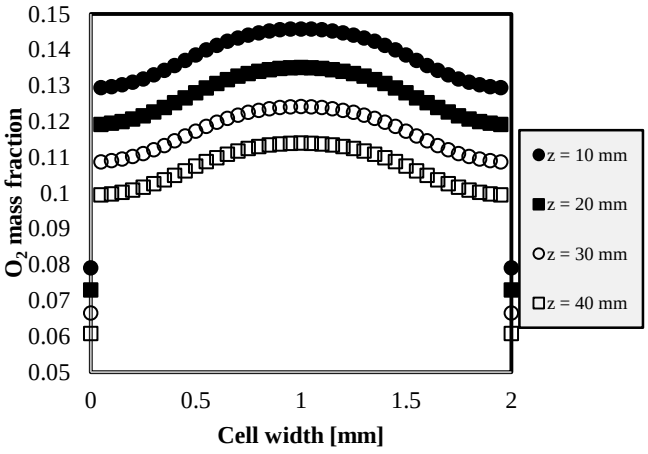

Voltage = 0.6

Figure 4. O_2 distribution in width of cell for four sections.

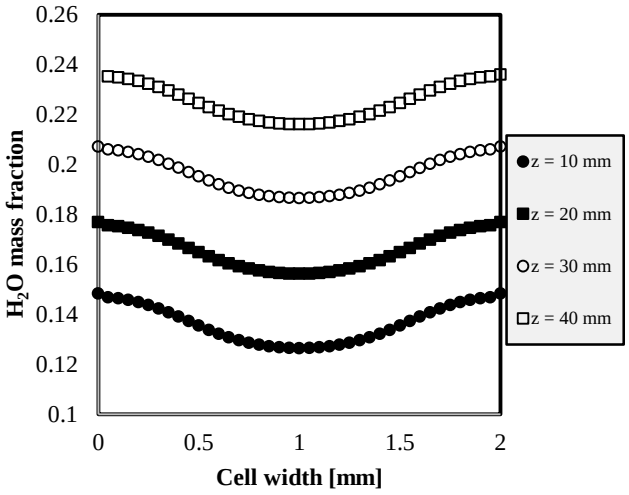

Voltage = 0.4

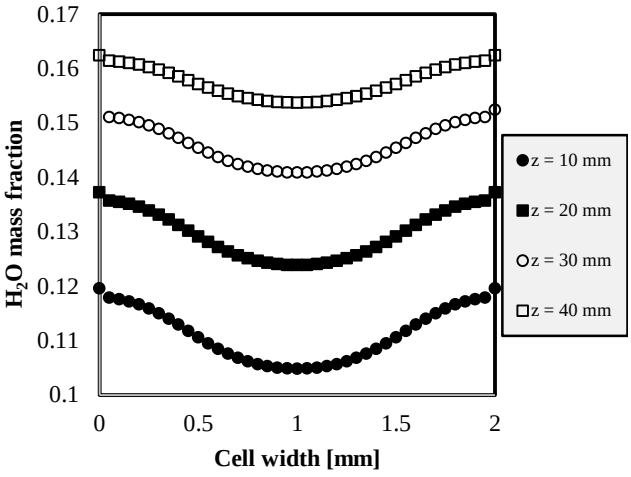

Voltage = 0.6

Figure 5. H_2O distribution in width of cell for four sections.

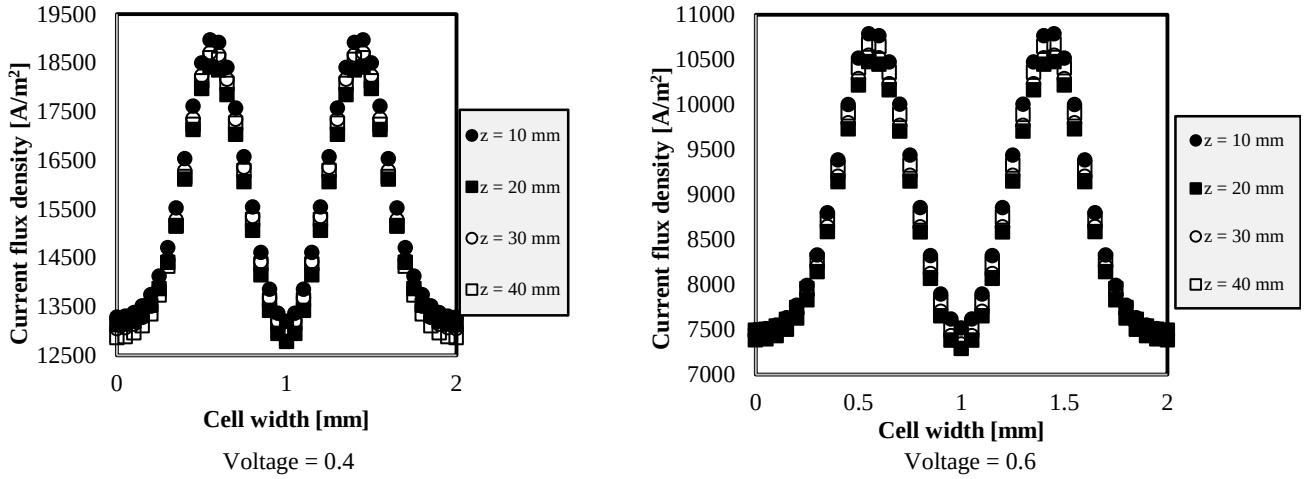

Figure 6. Current density distribution in width of cell for four sections.

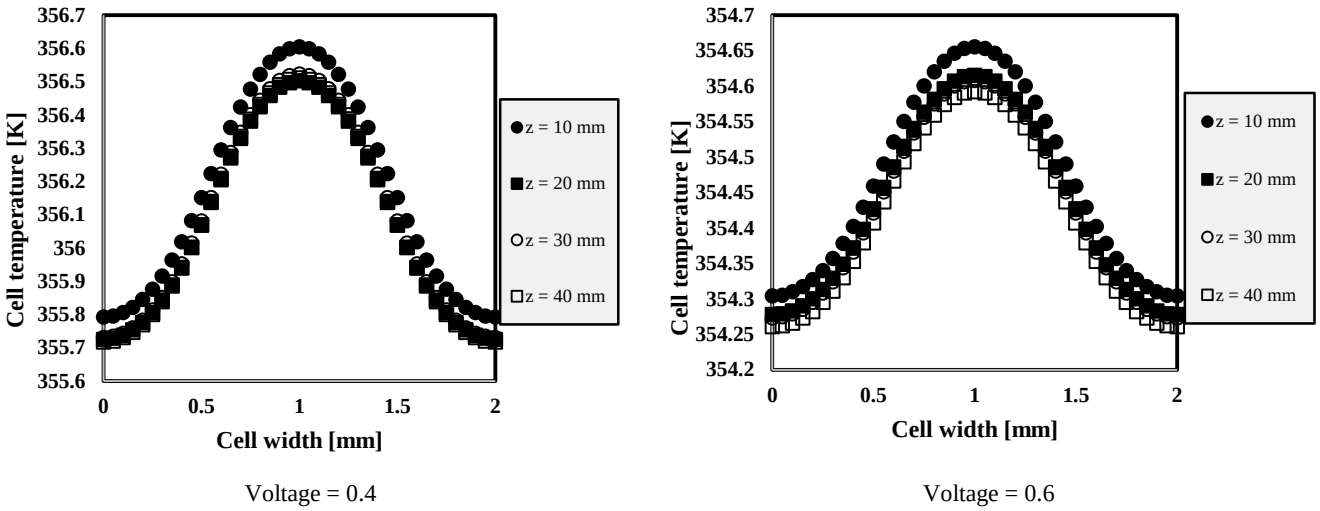

Figure 7. Temperature distribution in width of cell for four sections.

5.1. Novel structure of gas channel

In this work, as a new model, a wavy-shaped flow channel was simulated. Figure 8b shows a view of this geometry. This model includes 5 identical arcs through the channel. Figure 9 shows the geometrical characteristics of the novel model. Key parameters such as O_2 and H_2o mass fraction, cathode over potential, temperature, and protonic conductivity were calculated and compared with the results of the base model.

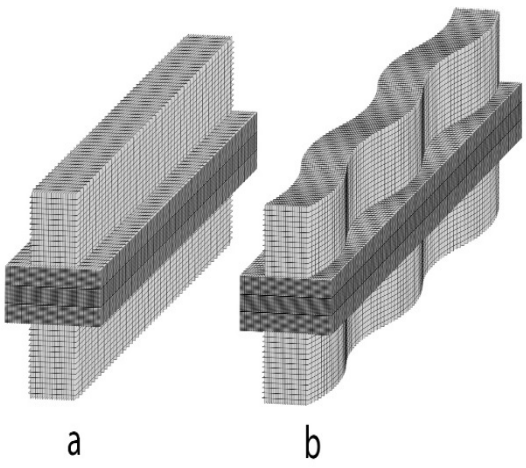

Figure 8. a) base model, b) model with wavy channels.

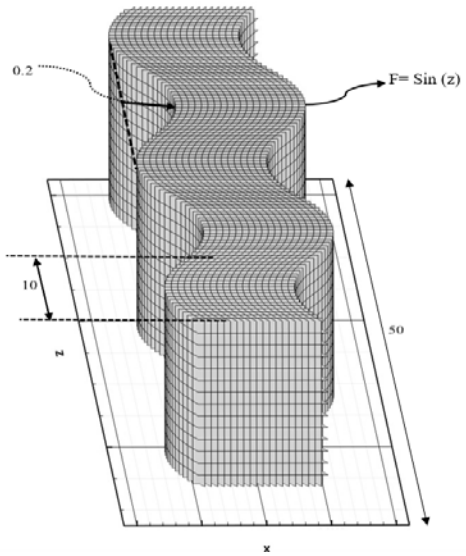

Figure 9. Geometric characteristics of a new model gas channel and its structured grid.

6. RESULTS AND DISCUSSION

Figure 10 shows that the new novel model experiences higher current density, especially at low cell voltages. Figure 11 illustrates an incredible decrease in O_2 mass fraction in a new structure at a cathode zone, meaning high O_2 consumption and, therefore, high H_2O production. Figure 13 shows this phenomenon. Because of high water level and more cooling effect in a new model, especially in bipolar regions, lower cell temperature is predictable, as demonstrated in Figure 15. Lengthening the species path from entering region toward the exit region of channels causes better diffusion of masses to the reaction area. Of note, in both models, the cell length is the same and equal to 50[mm].

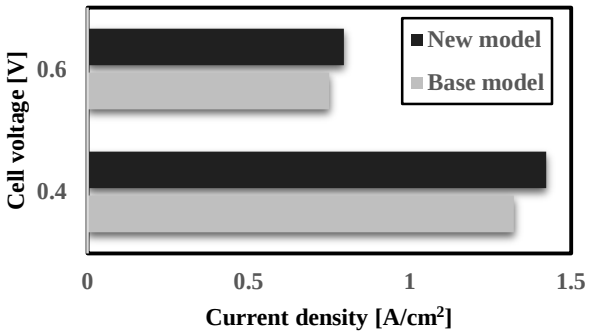

Figure 10. Current density for both models in two cell voltages.

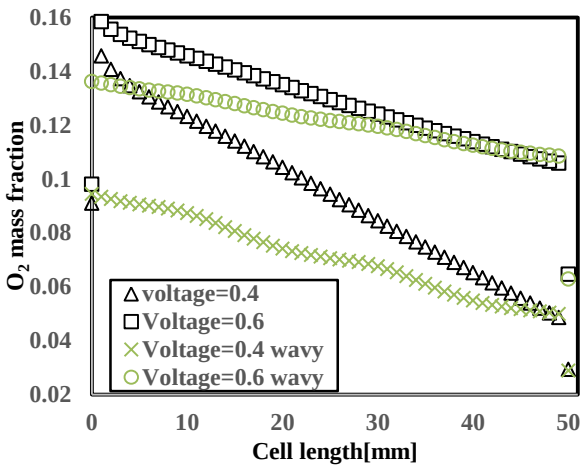

Figure 11. O_2 mass fraction at membrane and cathode catalyst layer interface for both models.

Figure 12 shows a uniform contour of O_2 mass fraction for the base model; however, the new model contour is completely different, especially for 0.6 V. In the new model, the shape of channel changes the species path from straight to wavy mode, which leads to more mass diffusion to the porous sections of the cell. In the base model, O_2 distribution is parabolic and it is observed in less amounts in shoulder regions, while it is highly distributed even in the middle points of the channel.

On the other hand, it is observed that O_2 consumption increases through the channel from entrance to exit in both models, which is the nature of the PEM fuel cells. Consequently, the water distribution according to the governing equations is the inverse of oxygen distribution (Figures 4 and 5). Therefore, water production in the novel model should be more than that in the base model, because the new model consumes more oxygen and hydrogen, as shown in Figure 13.

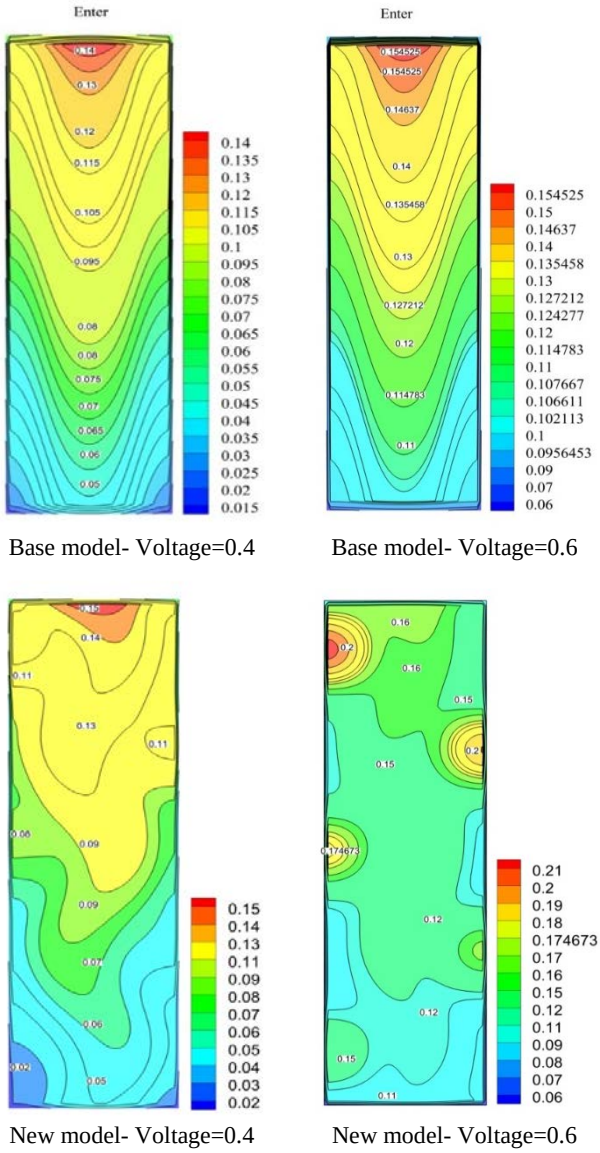

Figure 12. O_2 mass fraction contors at membrane and cathode catalyst layer interface for both models.

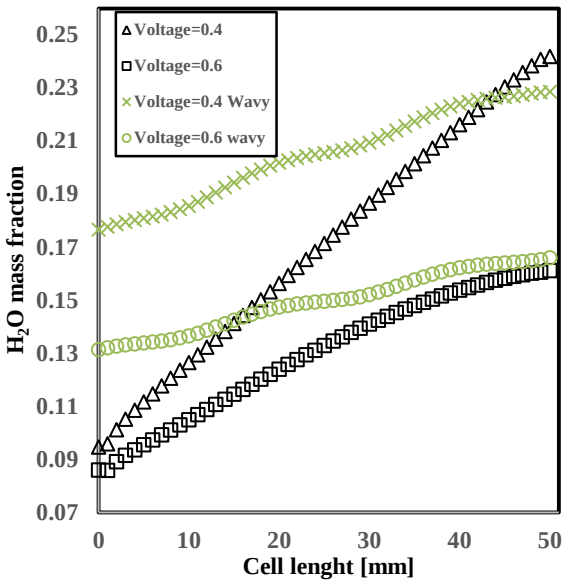

Figure 13. H_2O mass fraction at membrane and cathode catalyst layer interface for both models.

Figures 14 and 15 illustrate the 3D plots of oxygen and water distributions for V= 0.4 [V], respectively. The kind of mass distributions in these figures has been expressed before. As a result, the more the amount of water, the lower the cell temperature, as presented in Figures 16 and 17.

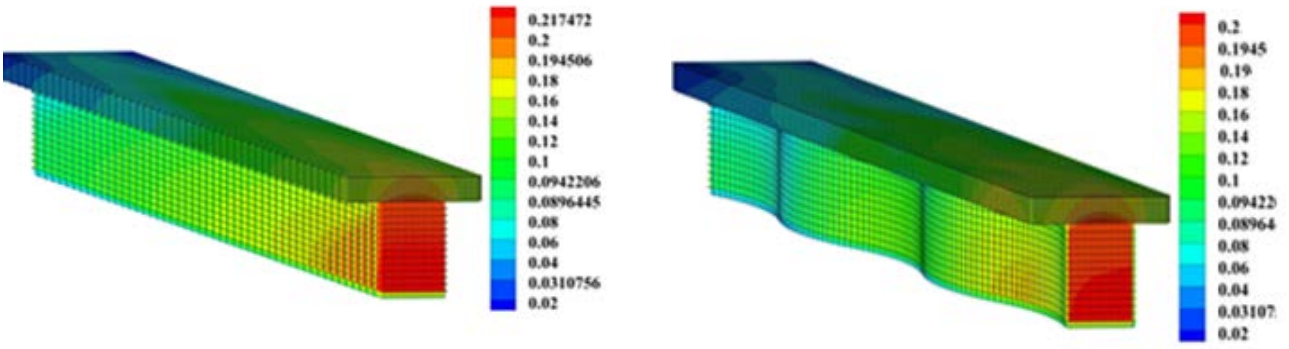

Figure 14. O_2 mass fraction at cathode channel and GDL-catalyst layers for both models.

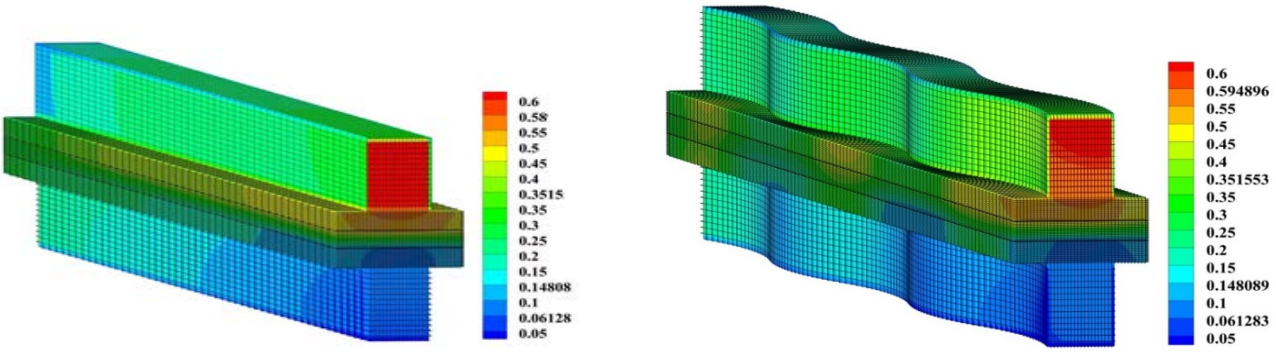

Figure 15. H_2O mass fraction at cathode and anode layers for both models.

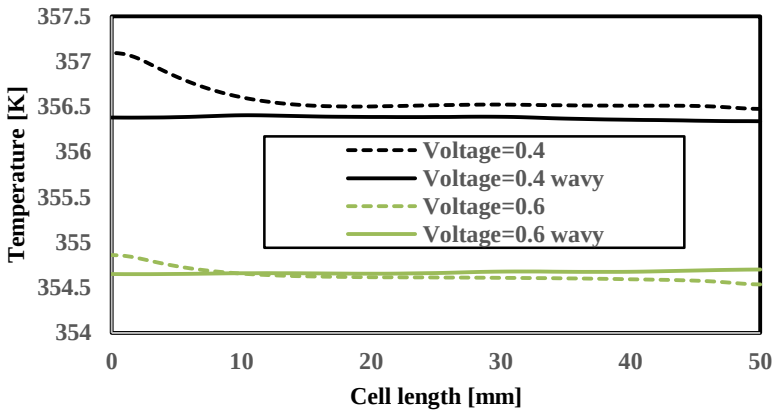

Figure 16. Cell Temperature at membrane and cathode catalyst layer interface for both models.

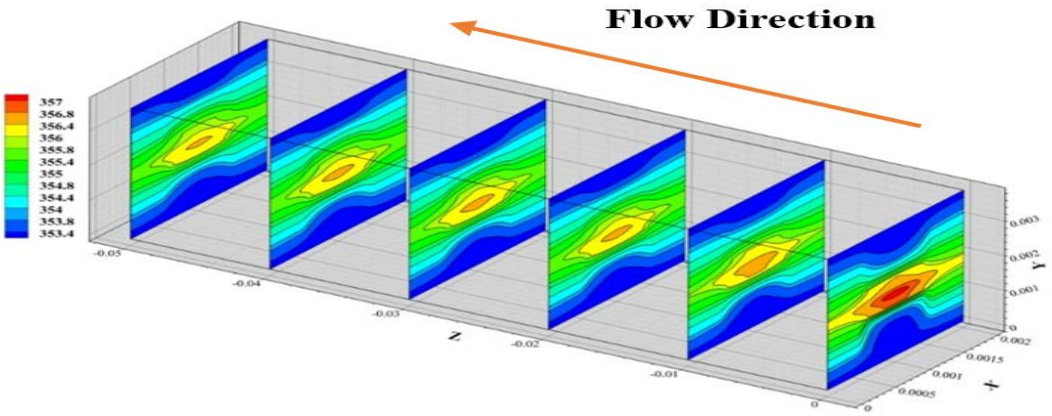

Base model- Voltage=0.4

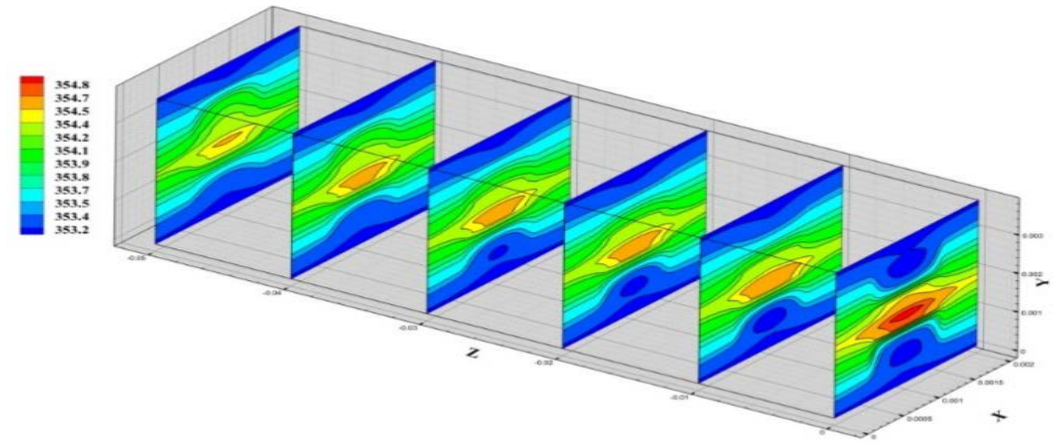

Base model- Voltage=0.6

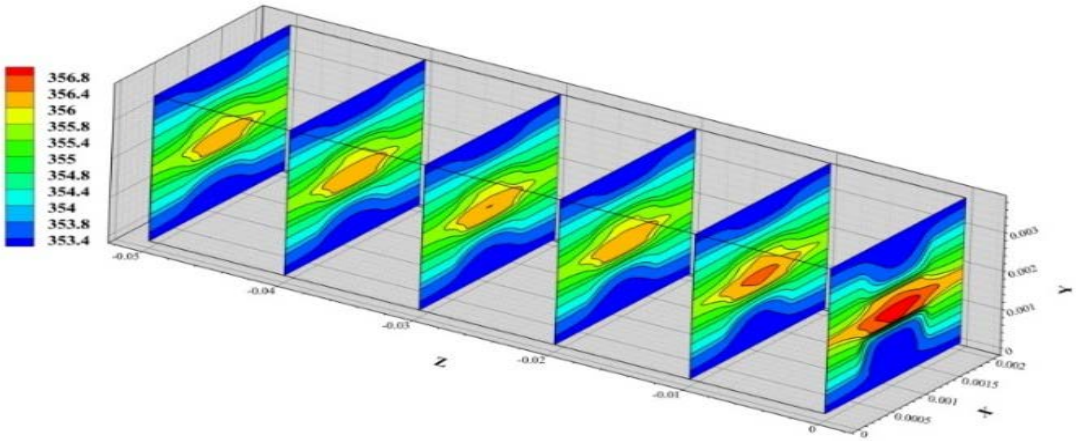

New model- Voltage=0.4

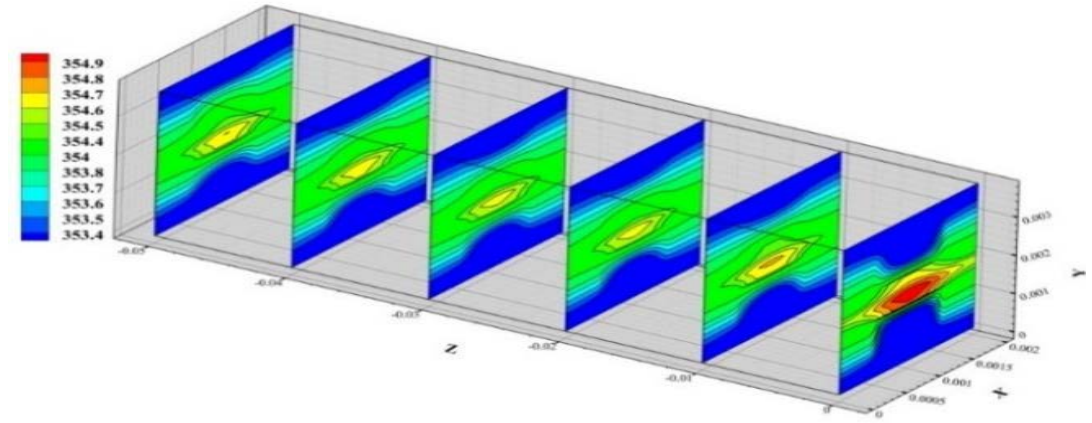

New model- Voltage=0.6

Figure 17. Temperature contours for both models.

Figures 18 to 20 show H_2 and H_2o mass fractions on the anode side of the cell regularly. These figures certify the previous mentioned expressions about the mass transport phenomenon.

While O_2 consumption and H_2O production for new geometry are more than those in a simple base model, it is implied here that H_2 consumption should be higher. Figure 19 shows contours of H_2 mass fraction, showing lower H_2 amount in the new model. The new model's contours are absolutely different. It is shown that there is a considerable H_2 consumption through the channel, implying greater efficiency.

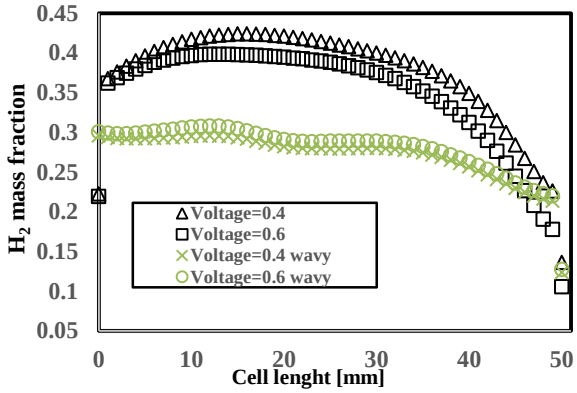

Figure 18. H_2 mass fraction at membrane and anode catalyst layer interface for both models.

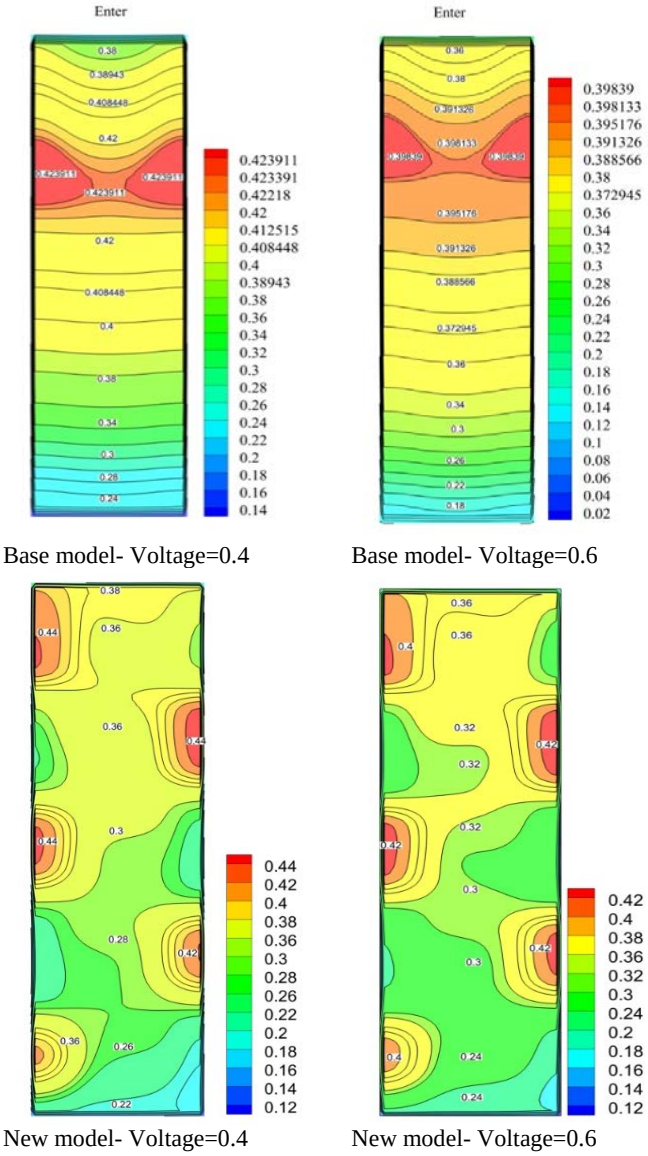

Base model- Voltage=0.4 Base model- Voltage=0.6

New model- Voltage=0.4 New model- Voltage=0.6

Figure 19. H_2 mass fraction contours at membrane and anode catalyst layer interface for both models.

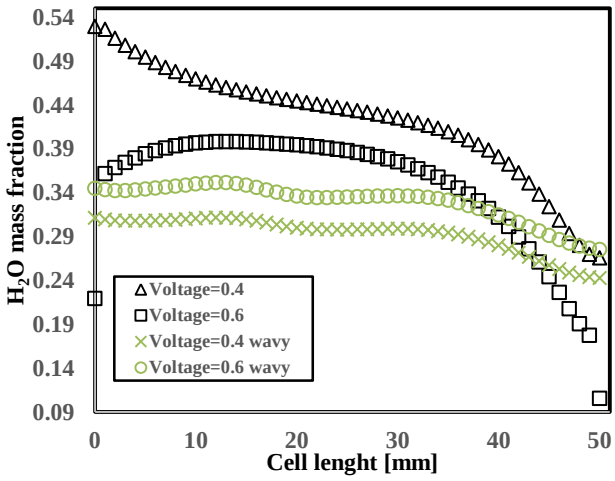

Figure 20. H_2O mass fraction at membrane and anode catalyst layer interface for both models.

Cathode Over Potential (COP) parameter is considerably related to the amount of O_2. The less oxygen, the more COP factor, which Figures 21 and 22 confirm each one. Therefore, along the cell, by decreasing the oxygen amount, the COP should increase. Another vital parameter, Cathode Protonic Conductivity (CPC), is strongly related to water distribution, as shown in Figure 23. Therefore, along the fuel cell, the amount of this property grows up. Of note, along the cell, the activity of water molecules to transfer the hydrogen toward the electrochemical reaction area is enhanced.

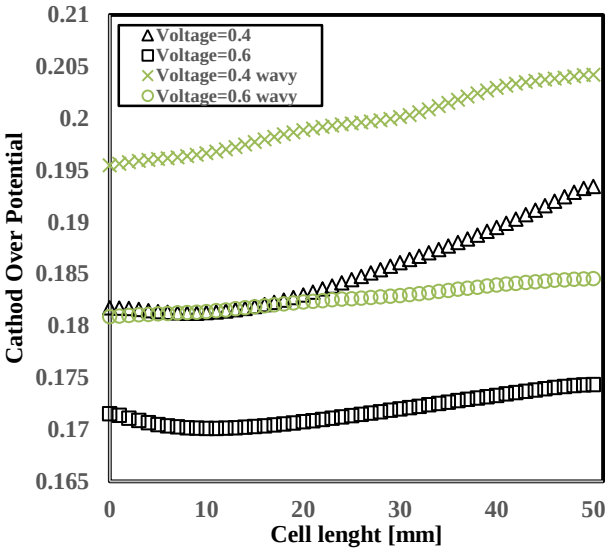

Figure 21. COP Parameter at membrane and cathode catalyst layer interface for both models.

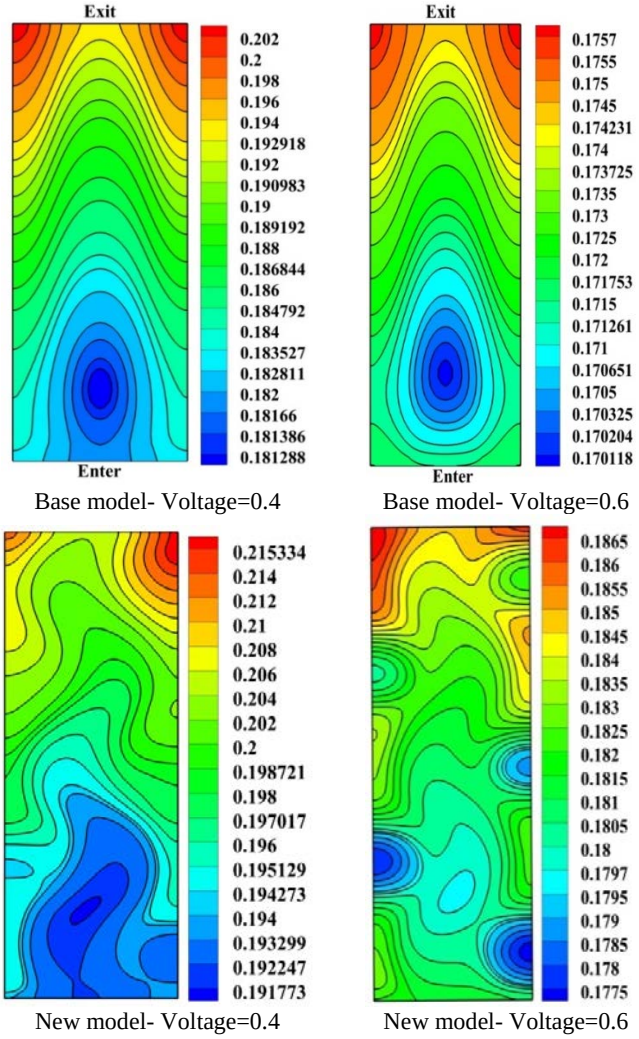

Base model- Voltage=0.4 Base model- Voltage=0.6

New model- Voltage=0.4 New model- Voltage=0.6

Figure 22. COP contour at membrane and cathode catalyst layer interface for both models.

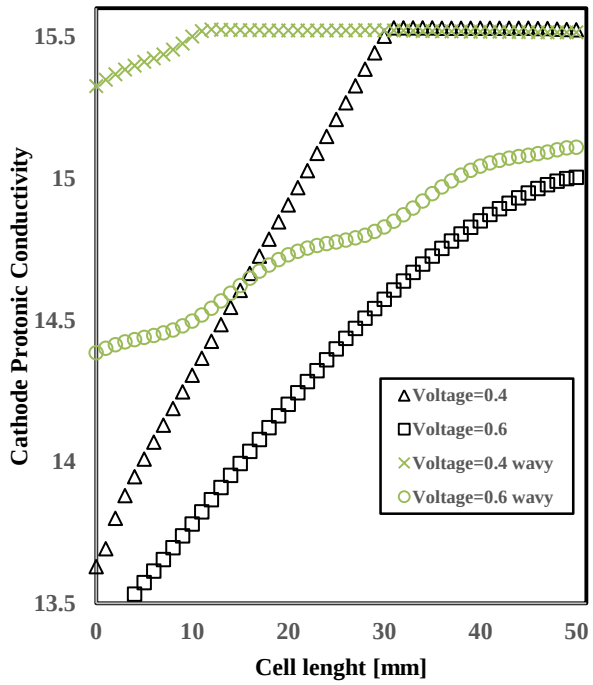

Figure 23. CPC parameter at membrane and cathode catalyst layer interface for both models.

The results showed that the current density in the new case study was higher than that of the base model. Figure 24 illustrates the comparison of the mentioned parameter for both models. There is a uniform trend for the base model and a periodic trend for the new model due to its geometry. It is clear that the mean values of new models' outputs are more than those of the base model. Figures 25 and 26 show the current density contours in an interface through the channel and cross-section in z = 25 mm, regularly.

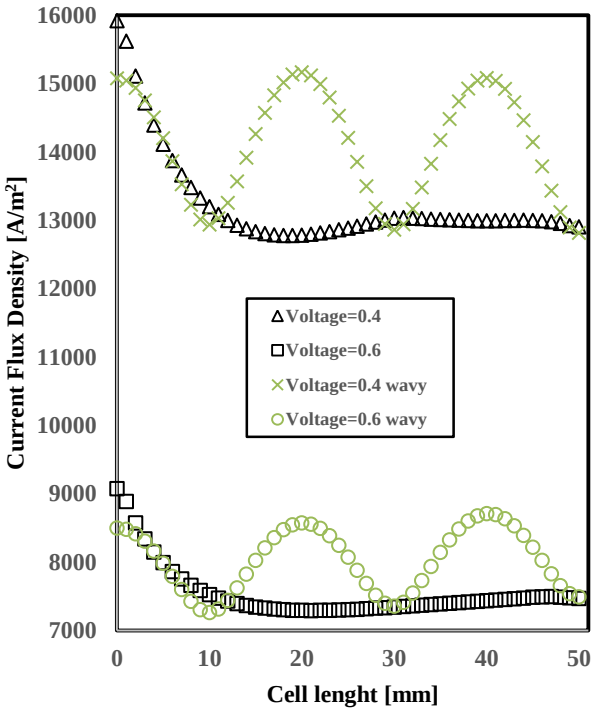

Figure 24. CFD parameter at membrane and cathode catalyst layer interface for both models.

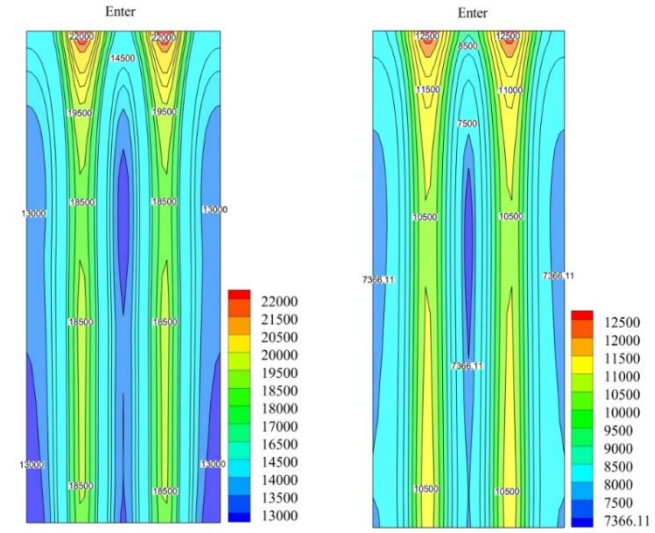

Base model- Voltage=0.4 Base model- Voltage=0.6

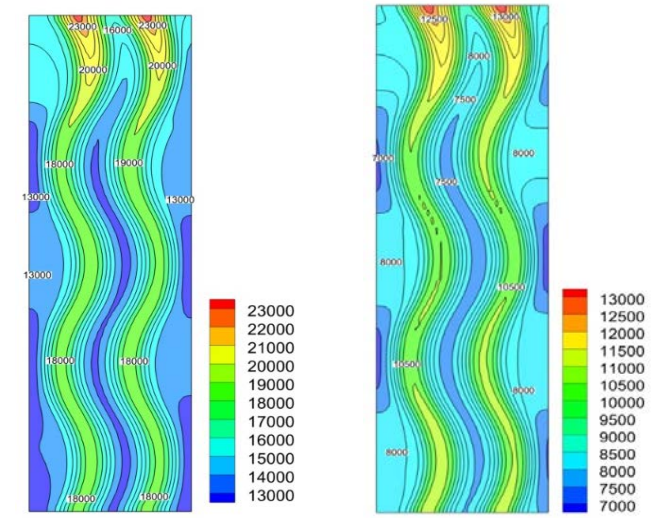

New model- Voltage=0.4 New model- Voltage=0.6

Figure 25. Current density for both models through cell length.

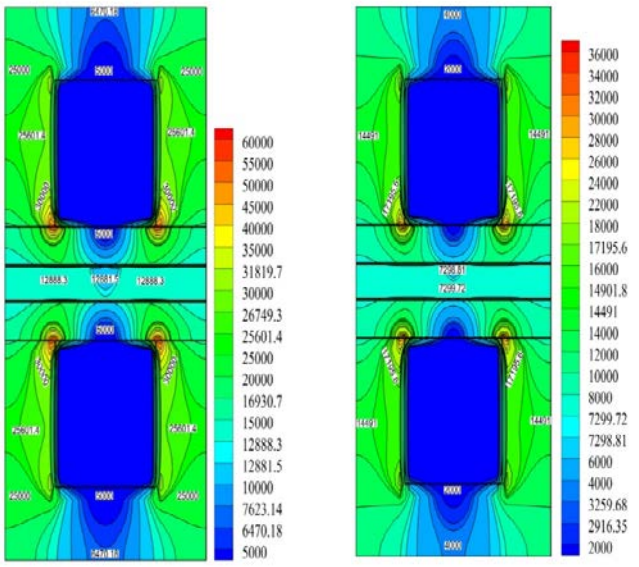

Base model- Voltage=0.4 Base model- Voltage=0.6

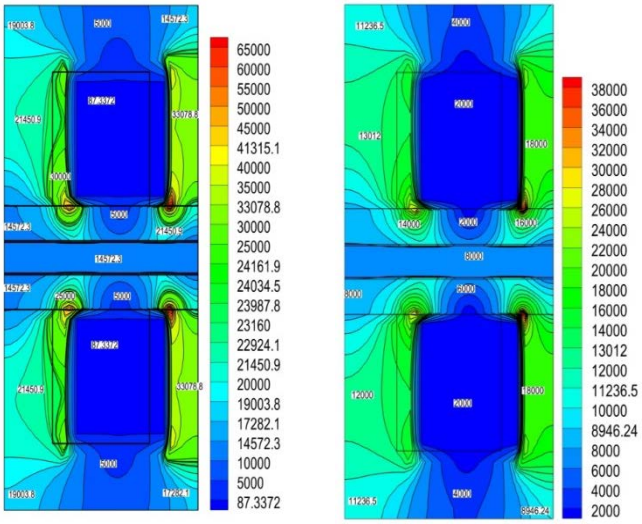

New model- Voltage=0.4 New model- Voltage=0.6

Figure 26. Current density for both models (section z=25 mm).

7. CONCLUSIONS

In the present work, a base conventional model and also the novel geometry for the gas channels were numerically simulated. Finite Volume Method for solving the governing equations was used, and the validation of numerical results against the experimental data was presented. Obtained results showed that the new model showed higher performance than the base conventional model, leading to somewhat more O_2 and H_2 consumption and also more water production in the new model. In other words, the new structure applied to gas channels resulted in more output current density, which is an important advantage of the proposed model. In doing so, since the path of the incoming species towards the cell gas channels can be elongated, their diffusion toward the electrochemical reaction area was enhanced, leading to higher current density extraction. It can be pointed out that more water production in the new model leads to cooling down the cell and decreasing the temperature distribution. Thus, the thermal stress and strain in cell layers can be neglected. Finally, a new proposed model of the fuel cell as a better case for its higher performance and the same cost against the base model can be introduced.

8. ACKNOWLEDGEMENT

We gratefully acknowledge Urmia University of Technology computer center manager for allowing us to use their computers.

NOMENCLATURE

a	Water activity
C	Molar concentration (mol m^{-3})
D	Mass diffusion coefficient (m^2 s^{-1})
F	Faraday constant (C mol^{-1})
I	Local current density (A m^{-2})
J	Exchange current density (A m^{-2})
K	Permeability (m^2)
M	Molecular mass (kg mol^{-1})
P	Pressure (Pa)
R	Universal gas constant (J mol^{-1} K^{-1})
T	Temperature (K)
t	Thickness (m)
U	Velocity vector (ms^{-1})
Vcell	Cell voltage (V)
Voc	Open-circuit voltage (V)
Greek letter	
α	Water transfer coefficient
ε^{eff}	Effective porosity
ρ	Density (kg m^{-3})
φ_e	Electrolyte phase potential (varies from −1 to 1) (v)
μ	Viscosity (kg m^{-1} s^{-1})
σ_m	Membrane conductivity (1 ohm^{-1} m^{-1})
η	Over potential (v)
λ_{eff}	Effective thermal conductivity (w m^{-1} k^{-1})
Subscripts and superscripts	
a	Anode
c	Cathode
Ch	Channel
k	Chemical species
m	Membrane
MEA	Membrane electrolyte assembly
ref	Reference value
sat	Saturated

REFERENCES

1. Kreuer, K.D., Ed., Fuel cells, Springer, New York, (2013). (https://doi.org/10.1007/978-1-4614-5785-5).
2. Bernardi, D.M. and Verbrugge, M.W., "Mathematical model of a gas diffusion electrode bonded to a polymer electrolyte", ***AIChE Journal***, Vol. 37, No. 8, (1991), 1151-1163. (https://doi.org/10.1002/aic.690370805).
3. Bernardi, D.M. and Verbrugge, M.W., "A mathematical model of the solid-polymer-electrolyte fuel cell", ***Journal of The Electrochemical Society***, Vol. 139, No. 9, (1992), 2477-2491. (https://doi.org/10.1149/1.2221251).
4. Fuller, T.F. and Newman, J., "Water and thermal management in solid-polymer-electrolyte fuel cells", ***Journal of The Electrochemical Society***, Vol. 140, No. 5, (1993), 1218-1225. (https://doi.org/10.1149/1.2220960).
5. Nguyen, T.V. and White, R.E., "Water and heat management model for proton-exchange-membrane fuel cells", ***Journal of The Electrochemical Society***, Vol. 140, (1993), 2178-2186. (https://doi.org/10.1149/1.2220792).
6. Dutta, S., Shimpalee, S. and Van Zee, J.W., "Three-dimensional numerical simulation of straight channel PEM fuel cells", ***Journal of Applied Electrochemical***, Vol. 30, (2000), 135-146. (https://doi.org/10.1023/a:1003964201327).
7. Berning, T. and Djilali, N., "Three-dimensional computational analysis of transport phenomena in a PEM fuel cell: A parametric study", ***Journal of Power Sourc***e, Vol. 124, (2003), 440-452. (https://doi.org/10.1016/s0378-7753(03)00816-4).
8. Yang, T.-H., Park, G.-G., Pugazhendhi, P., Lee, W.-Y. and Kim, C.S., "Performance improvement of electrode for polymer electrolyte membrane fuel cell", ***Korean Journal of Chemical Engineering***, Vol. 19, No. 3, (2002), 417-420. (https://doi.org/10.1007/bf02697149).
9. Molaeimanesh, Gh. and Akbari, M.H., "Water droplet dynamic behavior during removal from a proton exchange membrane fuel cell gas diffusion layer by Lattice-Boltzmann method", ***Korean Journal of Chemical Engineering***, Vol. 31, No. 4, (2014), 598-610. (https://doi.org/10.1007/s11814-013-0282-6).
10. Carral, Ch. and Mélé, P., "A numerical analysis of PEMFC stack assembly through a 3D finite element model", ***International Journal of Hydrogen Energy***, Vol. 39, No. 9, (2014), 4516-4530. (https://doi.org/10.1016/j.ijhydene.2014.01.036).
11. Ahmadi, N., Dadvand, A., Rezazadeh, S. and Mirzaee, I., "Analysis of the operating pressure and GDL geometrical configuration effect on PEM fuel cell performance", ***Journal of The Brazilian Society of Mechanical Science and Engineering***, (2016). (https://doi.org/10.1007/s40430-016-0548-0).
12. Rezazadeh, S. and Ahmadi, N., "Numerical investigation of gas channel shape effect on proton exchange membrane fuel cell performance", ***Journal of The Brazilian Society of Mechanical Sciences and Engineering***, (2015). (https://doi.org/10.1007/ s40430-014-0209-0).

13. Ticianelli, E.A., Derouin, C.R., Redondo, A. and Srinivasan, S., "Methods to advance technology of proton exchange membrane fuel cell", ***Journal of Electrochemical Society***, Vol. 135, No. 9, (1988), 2209-2214. (https://doi.org/10.1149/1.2096240).

14. Ahmadi, N., Pourmahmoud, N., Mirzaee I. and Rezazadeh, S., "Three-dimensional computational fluid dynamic study of effect of different channel and shoulder geometries on cell performance", ***Australian Journal of Basic and Applied Sciences***, Vol. 5, No. 12, (2011), 541-556.

15. Ahmadi, N., Rezazadeh, S., Mirzaee, I. and Pourmahmoud., N., "Three-dimensional computational fluid dynamic analysis of the conventional PEM fuel cell and investigation of prominent gas diffusion layers effect", ***Journal of Mechanical Science and Technology***, Vol. 26, No. 8, (2012), 2247-2257. (https://doi.org/10.1007/s12206-012-0606-1).

16. Wang, L., Husar, A., Zhou,T. and Liu, H., "A parametric study of PEM fuel cell performances", ***International Journal of Hydrogen Energy***, Vol. 28, No. 11, (2003), 1263-1272. (https://doi.org/10.1016/s0360-3199(02)00284-7).

17. Ahmadi, N., Rezazadeh, S. and Mirzaee, I., "Study the effect of various operating parameters of proton exchange membrane", ***Periodica Polytechnica. Chemical Engineering***, Vol. 59, No. 3, (2015), 221-235. (https://doi.org/10.3311/ppch.7577).

18. Ahmadi, N., Rezazadeh, S., Dadvand, A. and Mirzaee, I., "Modelling of gas transport in proton exchange membrane fuel cells", ***Institution of Civil Engineers (ICE)***, Vol. 170, No. 4, (2017), 163-179. (https://doi.org/10.1680/jener.15.00015).

19. Ahmadi, N., Rezazadeh, S., Dadvand, A. and Mirzaee, I., "Numerical investigation of the effect of gas diffusion layer with semicircular prominences on polymer exchange membrane fuel cell performance and species distribution", ***Journal of Renewable Energy and Environment (JREE)***, Vol. 2, No. 2, (2015), 36-46.

20. Rezazadeh, S., Mirzaee, I., Pourmahmoud and Ahmadi, N., "Three dimensional computational fluid dynamics analysis of a proton exchange membrane fuel cell", ***Journal of Renewable Energy and Environment (JREE)***, (2014).